Combustion, Explosion, and Shock Waves, Vol. 35, No. 3, 1999

Equilibrium and Kinetic Modeling of High-Pressure Pyrolysis and Oxidation of Hydrocarbons

N. A. Dvornikov[1]

UDC 536.46+66.093

Translated from *Fizika Goreniya i Vzryva*, Vol. 35, No. 3, pp. 20–28, May–June 1999.
Original article submitted May 15, 1998; revision submitted October 28, 1998.

The pyrolysis and incomplete oxidation of hydrocarbons in the presence of water at high pressures is modeled numerically. The calculations show that the nonidealness of the gas can have a significant effect on the composition and temperature of the reaction products. The results of equilibrium and global kinetics calculations are in better agreement with one another, but a model with detailed kinetics fits the experimental data better.

CHEMICAL EQUILIBRIUM CALCULATION

The method for calculating the equilibrium composition in the course of the chemical transformations is based on the fact that at the chemical equilibrium point, the Gibbs energy has a minimum. For real systems the specific Gibbs energy can be written in the form [1]

$$G = \sum_{j=1}^{NS} g_i n_i. \tag{1}$$

Here n_i is the number of moles of material i in the volume, NS is the number of substances in all phases (substances with the same atomic composition but in different phases have different subscripts i), g_i is the chemical potential per mole of substance i including mixing, with

$$g_i = h_i^0 - Ts_i^0 + RT\Big[\ln\frac{p}{p_0} + \ln\frac{n}{\sum\limits_k n_k} + \ln f_i\Big], \tag{2}$$

where h_i^0 and s_i^0 are the specific enthalpy and entropy at standard pressure $p_0 = 1$ atm, which are functions of the temperature T for each of the substances, R is the universal gas constant, p is the pressure at which the equilibrium for the gases is sought with $p = p_0$ for liquids and solids, and f_i is the fugacity [2]. In all the following calculations, the pressure in the system will be assumed constant, $p = \text{const}$. For solutions and gaseous mixtures, the sum in $\sum_k n_k$ is taken over all substances of that phase to which substance i belongs, while for pure components $\sum_i n_i = n_i$. For an ideal gas, the fugacity is $f_i = 1$. The fugacity of real gases was determined using the Redlich–Quang equation of state:

$$p = \frac{RT}{V-b} - \frac{d}{T^{0.5}V(V+b)}, \tag{3}$$

where d and b are constants and V is the molar volume. With this equation, the expression for the fugacity can be written in the form [2]

$$\ln f_i = \ln\frac{V}{V-b} + \frac{b_i}{V-b} - \ln Z + \frac{db_i}{b^2RT^{1.5}}\Big(\ln\frac{V+b}{V} - \frac{b}{V+b}\Big) - \frac{2\sum\limits_j x_j d_{ij}}{bRT^{1.5}}\ln\frac{V}{V+b},$$

where $x_i = n_i/\sum_k n_k$ is the number of moles of substance i per mole of the gaseous mixture, Z is the compressibility, and $d_{ij} = \sqrt{d_i}\sqrt{d_j}$ is determined from the coefficients d in the equation of state for the pure substances with subscripts i and j.

The functional (1) is minimized with the following constraints:

(1) Conservation of the number of atoms of species j:

$$\sum_{i=1}^{NS} a_{ji} n_i = e_i \quad (j = 1, NL) \tag{4}$$

---

[1] Institute of Thermal Physics, Siberian Division, Russian Academy of Sciences, Novosibirsk 630090.

Here a_{ji} is the number of atoms of species j in substance i, e_i is the total number of atoms of species j, and NL is the number of atomic species in the system.

(2) The change in the enthalpy of the system including losses into the surroundings:

$$\sum_{i=1}^{NS} h_i n_i + DH = \sum_{i=1}^{NS} h_i^0 n_i^0 + DH^0 - Q, \qquad (5)$$

where h_i is the enthalpy neglecting the nonidealness of the gas, DH is the change in enthalpy owing to the real properties of the gas, Q is the heat loss by the system into the surroundings, and the superscript 0 denotes inlet conditions. With the Redlich–Quang equation of state,

$$DH = \frac{bRT}{V-b} - \frac{d}{T^{0.5}(V+b)} - \frac{3d}{2bT^{0.5}} \ln \frac{V+b}{V}. \qquad (6)$$

(3) The inequality

$$n_i \geqslant 0 \qquad (7)$$

is satisfied.

The problem of minimizing (1) with the constraints (4), (5), and (7) is equivalent to iterative minimization of (1) with constraints (4) and (7) for a fixed temperature at each step of determining the composition and determining the temperature using Eq. (5) for a fixed composition. This simplifies the mathematical transformations in minimizing the functional

$$F = \sum_{i=1}^{NS} n_i g_i + \sum_{j=1}^{NL} \lambda_j \Big(\sum_{i=1}^{NS} a_{ji} n_i - b_j \Big), \qquad (8)$$

since there is no need to include the temperature dependence of this functional.

The extrema were determined by Newton's method using undetermined Lagrange multipliers π_j. At each step the iteration procedure yielded corrections for the concentrations from Eq. (8):

$$\Delta \ln(n_i) = -\sum_{k=1}^{NL} \Delta\pi_k a_{ki} - \Big(c_i + \ln \frac{n_i}{m_L} + \sum_{j=1}^{NL} \pi_j a_{ji} \Big), \qquad (9)$$

where

$$\pi_j = \frac{\lambda_j}{RT}, \qquad c_i = \frac{h_i^0 - Ts_i^0}{RT} + \ln \frac{p}{p_0} + \ln f_i,$$

$m_L = \sum_k n_k$ is the sum of the concentrations of all the substances in the phase L, to which the substance i belongs. For pure components, we have $m_L = n_i$. Here we have assumed [1] that $\partial c_i / \partial n_i = 0$, while $m_L = \mathrm{const}$ corresponds to an equilibrium state.

For the correction to the Lagrange multipliers $\Delta\pi_k$, besides Eq. (9), the following procedure was developed for minimizing the conservation functional (4) for the number of atoms:

$$\sum_{i=1}^{NS} a_{ji} n_i \Delta \ln n_i = -\Big(\sum_{i=1}^{NS} a_{ji} n_i - e_j \Big), \qquad (10)$$

from which the corrections to the Lagrange multipliers were determined:

$$\sum_{k=1}^{NL} \Delta\pi_k \sum_{i=1}^{NS} a_{ki} a_{ji} n_i = \Big(\sum_{i=1}^{NS} a_{ji} n_i - e_j \Big) - \sum_{i=1}^{NS} a_{ji} n_i \Big(c_i + \ln \frac{n_i}{m_L} + \sum_{k=1}^{NL} \pi_k a_{ki} \Big), \quad j = 1, NL. \qquad (11)$$

On solving the NL equations of (11) for the NL unknown $\Delta\pi_k$, it is possible to determine the corrections to the concentrations of the substances $\Delta \ln n_i$ from Eqs. (9). Given these corrections, we have

$$\pi_j^{t+1} = \pi_j^t + \alpha \Delta \pi_j, \qquad \ln(n_i)^{t+1} = \ln(n_i)^t + \alpha \Delta \ln(n_i), \qquad (12)$$

where the superscript t denotes the iteration number and α is the relaxation coefficient. After this, the concentrations of each of the substances n_i were calculated and, then, the masses of each of the phases, including the individual components. The correction to the temperature corresponding to the new distribution of the concentrations u can then be calculated using Eq. (5):

$$\Delta T = \frac{\Big(\sum_{i=1}^{NS} h_i n_i^0 + DH^0 - Q \Big) - \Big(\sum_{i=1}^{NS} h_i n_i + DH \Big)}{c_p}, \qquad (13)$$

Here c_p is the specific heat of the entire mixture at constant pressure under these conditions. Given the correction

$$T^{t+1} = T^t + \alpha \Delta T. \qquad (14)$$

After establishment of a new temperature in the system, the calculations are performed using Eqs. (9)–(14).

MODEL WITH GLOBAL KINETICS

1. We assume that the fraction of the initial hydrocarbon in the system varies in accordance with kinetic equations, while all other substances, including the reaction products and oxygen, are in a state of chemical equilibrium.

2. The amount of hydrocarbon in the system varies through two global reactions. The pyrolysis reaction is a decomposition of the initial hydrocarbon into its simplest constituents:

$$\mathrm{C}_x\mathrm{H}_y + \mathrm{M} \Longrightarrow \text{Products} + \mathrm{M}. \tag{15}$$

The second global reaction producing a change in the concentration of the initial hydrocarbon is its oxidation [3]:

$$\mathrm{C}_x\mathrm{H}_y + \left(\frac{x}{2} + \frac{y}{4}\right)\mathrm{O}_2 \Longrightarrow x\mathrm{CO} + \frac{y}{2}\mathrm{H}_2\mathrm{O}. \tag{16}$$

Since preliminary calculations show that, in equilibrium, heavy hydrocarbons are entirely transformed into lighter components, we only consider the rate of the direct reactions leading to disappearance of the heavy hydrocarbons.

These assumptions make it possible to determine the time required for conversion of the hydrocarbon, but they do not take the actual kinetics of the reaction products into account. The kinetic equations for the gaseous phase are examined in the third model.

MODEL WITH DETAILED KINETICS FOR THE GASEOUS PHASE REACTIONS

We shall examine the equations for the formal reaction kinetics in the gaseous phase in more detail, taking into account the nonidealness of the equations of state,

$$\sum_i \nu'_{ij} A_i \Longleftrightarrow \sum_i \nu''_{ij} A_i. \tag{17}$$

According to the law of mass action, the rate of change of the amount of substance i in the forward direction of reaction j is determined by the equation [4]

$$w^+_{ij} = (\nu''_{ij} - \nu'_{ij}) k^+_j \prod_k C_k^{\nu'_{kj}}. \tag{18}$$

For the reverse reaction, we have

$$w^-_{ij} = (\nu'_{ij} - \nu''_{ij}) k^-_j \prod_k C_k^{\nu''_{kj}}. \tag{19}$$

Here ν'_{ij}.and ν''_{ij} are the stoichiometric coefficients for the forward and reverse reactions, C_k is the molar-volume concentration, and k^+_j and k^-_j are the rate constants for the forward and reverse reactions. When there are reactions with a third body (the gas), instead of C_k (the molar-volume concentration of the third body), on puts the sum of C_k over all the gases in Eqs. (18) and (19).

Given the principle that the elementary reactions proceed independently of one another, the total rate of change of the amount of substance i is equal to the sum of the rates of change of the amount of this material in all the reactions:

$$\frac{1}{V}\frac{dn_i}{d\tau} = w_i = \sum_j w^+_{ij} + \sum_j w^-_{ij}, \tag{20}$$

(τ is the reaction time). Multiplying and dividing the left hand side of Eq. (20) by the mass M of the entire gas in volume V, and noting that the molar-mass concentration is $\sigma_i = n_i/M = C_i/\rho$, where ρ is the density of the mixture of substances in the gaseous phase and M and V are the mass and volume of this phase, from Eqs. (20) with Eqs. (18) and (19) we obtain an equation for the time variation of the molar-mass concentration for an ideal displacement reactor [4]:

$$\frac{d\sigma_i}{d\tau} = \sum_j (\nu''_{ij} - \nu'_{ij}) k^+_j \rho^{\sum\limits_k \nu'_{kj} - 1} \prod_k \sigma_k^{\nu'_{kj}}$$

$$- \sum_j (\nu''_{ij} - \nu'_{ij}) k^-_j \rho^{\sum\limits_k \nu''_{kj} - 1} \prod_k \sigma_k^{\nu''_{kj}}. \tag{21}$$

From Eqs. (18) and (19), together with the condition that the sum of the rates of change in the amount of substance i in the forward and reverse reactions equals zero, we obtain the equilibrium constant K_j for reaction j:

$$K_j = \frac{k^+_j}{k^-_j} = \frac{\prod\limits_k C_k^{\nu''_{kj}}}{\prod\limits_k C_k^{\nu'_{kj}}} = \frac{\rho^{\sum\limits_k \nu''_{kj}} \prod\limits_k \sigma_k^{\nu''_{kj}}}{\rho^{\sum\limits_k \nu'_{kj}} \prod\limits_k \sigma_k^{\nu'_{kj}}}. \tag{22}$$

The relationship between the rate constants for real and ideal gases can be established through a determination of the equilibrium in terms of the chemical potentials. It is known that in a state of chemical equilibrium the difference between the chemical potentials for the reagents of reaction (17) to the left and right is equal to zero [5]:

$$\Delta_j g = \sum_i (\nu''_{ij} - \nu'_{ij}) g_i = 0. \tag{23}$$

Here g_i is determined from Eq. (2). Dividing Eq. (23) by RT, we obtain

$$\sum_i (\nu''_{ij} - \nu'_{ij}) \left(\ln \frac{p}{p_0} + \ln \frac{n_i}{\sum\limits_k n_k} + \ln f_i \right)$$

$$= - \sum_i (\nu''_{ij} - \nu'_{ij}) \frac{h^0_i - T s^0_i}{RT}. \tag{24}$$

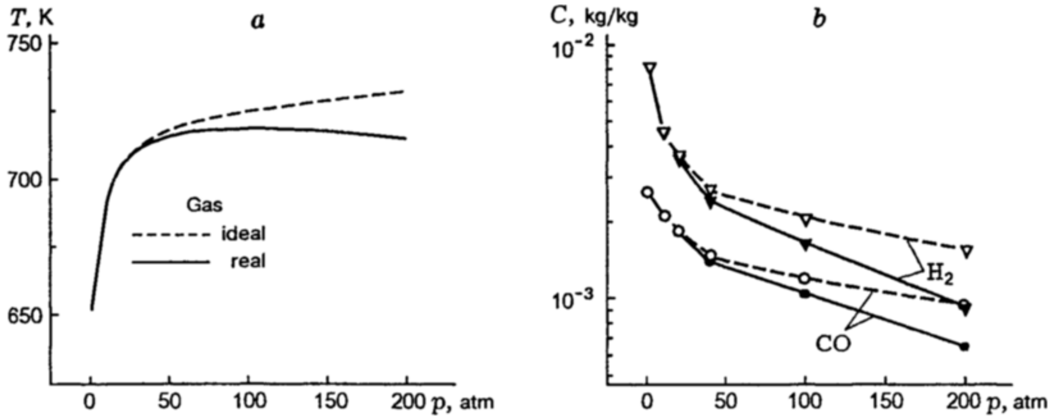

Fig. 1. Variations in the reactor temperature (a) and in the mass concentrations of CO and H_2 (b) during gasification of carbon in water.

The quantity $\sum_i(\nu''_{ij} - \nu'_{ij})(h_i^0 - Ts_i^0) = \Delta_j g^0$ is referred to as the change in the standard Gibbs energy of reaction j. Given that $\frac{n_i}{\sum n_k} = \frac{\sigma_i}{\sum \sigma_k}$, while $p = \frac{\rho}{\mu} RTZ$, where $\mu = \frac{1}{\sum_i \sigma_i}$ is the molecular mass of the gas, we can rewrite Eq. (24) in the form

$$\left(\frac{p\mu}{p_0}\right)^{\sum_i(\nu'_{ij}-\nu''_{ij})} \exp\left(-\frac{\Delta_j g^0}{RT}\right) = \frac{\prod_i(\sigma_i f_i)^{\nu''_{ij}}}{\prod_i(\sigma_i f_i)^{\nu'_{ij}}} \quad (25)$$

or

$$\frac{\prod_i(f_i)^{\nu'_{ij}}}{\prod_i(f_i)^{\nu''_{ij}}} \left(\frac{RTZ}{p_0}\right)^{\sum_i(\nu'_{ij}-\nu''_{ij})} \exp\left(-\frac{\Delta_j g^0}{RT}\right)$$

$$= \frac{\rho^{\sum_i \nu''_{ij}} \prod_i(\sigma_i)^{\nu''_{ij}}}{\rho^{\sum_i \nu'_{ij}} \prod_i(\sigma_i)^{\nu'_{ij}}}. \quad (26)$$

If we assume that the law of mass action is valid at high pressures, as well, then Eq. (22) for the reaction rates, which was derived from the law of mass action, coincides with the right hand side of Eq. (26), which was obtained by equating the Gibbs energies before and after the reaction in chemical equilibrium. This makes it possible to calculate the equilibrium constant from the left hand side of Eq. (26) and then to determine the rate of the reverse reaction if the forward reaction rate is known. Here, assuming that the left-to-right reaction rate constant depends only on the parameters on the left side, while the right-to-left reaction rate depends on the parameters on the right, on comparing Eqs. (22) and (26) we obtain

$$k_j^+ = k_{0j}^+ Z^{\sum_i \nu'_{ij}} \prod_i (f_i)^{\nu'_{ij}}. \quad (27)$$

Similarly, the rate constant for the reverse reaction is

$$k_j^- = k_{0j}^- Z^{\sum_i \nu''_{ij}} \prod_i (f_i)^{\nu''_{ij}}. \quad (28)$$

The forward reaction rate constant for an ideal gas can be written in the Arrhenius form

$$k_{0j}^+ = A_j T^{n_j} \exp(-T_{aj}/T), \quad (29)$$

where A_j, n_j, and T_{aj} are constants. The reverse reaction rate constant for an ideal gas is related to that for the forward reaction by

$$k_{0j}^- = k_{0j}^+ \left(\frac{RT}{p_0}\right)^{\sum_i(\nu''_{ij}-\nu'_{ij})} \exp\frac{\Delta_j g^0}{RT}. \quad (30)$$

Equation (30) is obtained from Eq. (22) and (26)–(28) and is well known for ideal gases [5]. Reaction rate constants in the forms (27)–(30) can be used to obtain an expression for the equilibrium constant in the form (26). In calculating the detailed kinetics of hydrocarbon conversion, here we have used Eq. (21) and the rate constants (27) and (28). The values of the constants in Eq. (29) were taken from published data [3, 6–11] and the reverse reaction rate constants were calculated using the thermodynamic properties of the reagents. Although a dependence of the reaction rate constants on the fugacity (activity) of the form (27) and (28) has been known for more than 60 years, these are used extremely rarely in practical calculations.

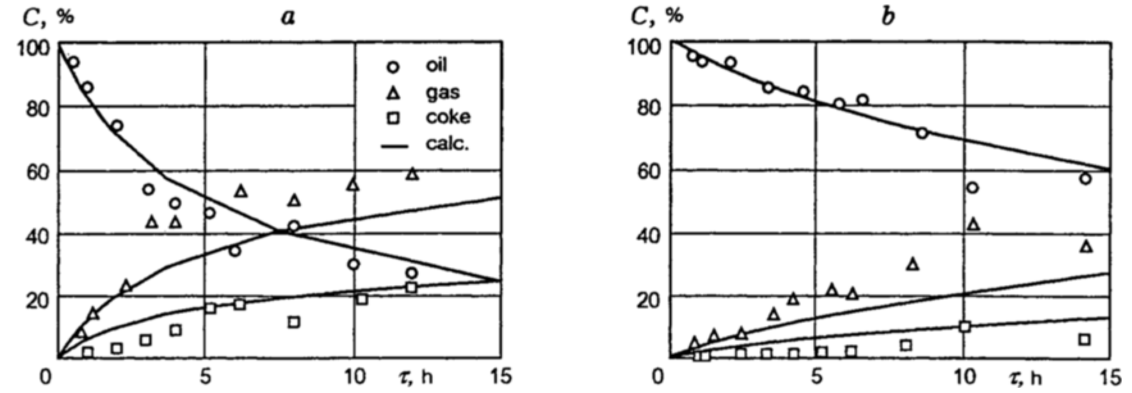

Fig. 2. Molar composition of the pyrolysis products of oil at $T = 683$ (a) and 663 K (b), $p = 1$ atm: points are experimental data from [8] and curves are calculated.

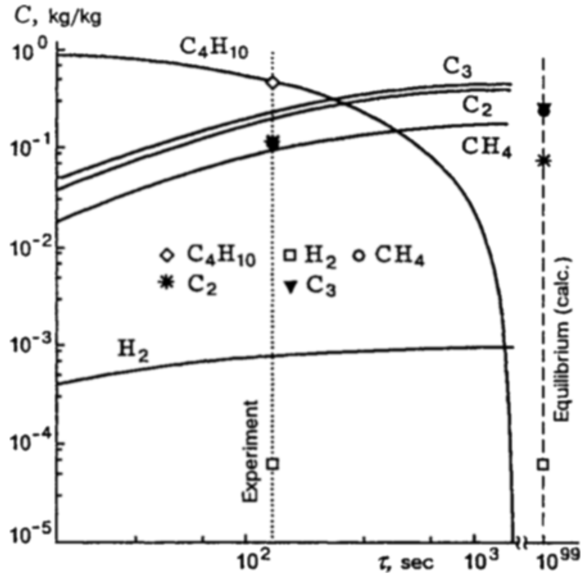

Fig. 3. Pyrolysis of butane at $p = 160$ atm.

It should be noted that, since the fugacities (activity for liquids) of the substances and the compressibility of the mixture depend on the concentrations of the substances the mixture, it is logical to eliminate them from the reaction rate constants. In this case, the law of mass action acquires a generalized form: the rate of the chemical reaction is proportional to the products of the concentrations times the fugacities (activities) times the compressibilities raised to the stoichiometric coefficients of the reagents:

$$w_{ij}^{+} = (\nu''_{ij} - \nu'_{ij}) k_{0j}^{+} \prod_{k} (C_k f_k Z)^{\nu'_{kj}}.$$

COMPUTATIONAL RESULTS

The results of some calculations of the gasification of a carbon in water (mass ratio 1 : 4) according to the chemical equilibrium model and using the equation of state of ideal and real gases are shown in Fig. 1. The inlet temperature is 800 K. The reaction was assumed to be adiabatic. It is evident that, despite the high temperature level, the difference in the calculations with the ideal and real models can be substantial. It should be noted that the ideal model calculations are the same as those using the ASTRA-4 model [12].

As a test we have done calculations on the pyrolysis of oil using the model with global kinetics described before. The data in Fig. 2 were obtained for reactor temperatures that differ by only 20 K, but the computational model and the experiment both yield substantial differences in the rate of pyrolysis for the two cases. A comparison of the computations and experiment shows that a kinetic model with a global pyrolysis reaction satisfactorily predicts both the pyrolysis time and the fractions of gaseous and solid reaction products.

The accuracy of the detailed kinetic model was determined for the example of the pyrolysis of butane. Two detailed kinetics models were used. In model I, 124 reactions among 24 substances were considered C_2H, C_2H_2, C_2H_3, C_2H_4, C_2H_5, C_2H_6, C_3H_4, C_3H_5, C_3H_6, C_3H_7, C_3H_8, C_4H, C_4H_{10}, C_4H_2, C_4H_3, C_4H_6, C_4H_7, C_4H_8, C_4H_9, CH_2, CH_3, CH_4, H, and H_2.

In model II, 250 reactions among 36 substances were considered, with the following species added to the previous list: C_5H_{10}, C_5H_{11}, C_5H_9, C_5H_{12}, C_6H_6, C_6H_{10}, C_6H_{11}, C_6H_{12}, C_6H_{13}, C_6H_{14}, C_7H_{14}, and C_7H_{16}. The kinetic data were taken from [3, 6, 13]. Table 1 compares calculations using models I and II

TABLE 1

Parameter	Experiment [11]	Calculation [13]	Model I	Model II
τ, sec	132	75	144	72
Butane conversion, mass%	56.98	56.2	56.6	57.2
H_2	0.06	0.003	0.075	0.004
CH_4	10.48	7.1	9.45	10.4
C_2	10.9	5.3	20.9	17.9
C_3	10.97	8.5	24.1	8.2
C_4	45.35	49.7	43.7	42.8
C_5	4.64	4.3	Not in list	12.0
C_6	5.15	20.9	–//–	7.9
C_7	8.41	3.6	–//–	0
Heavy products	8.7	Not in list	–//–	Not in list

TABLE 2

Molar composition, %	[6], τ=1.07 sec		This paper		
	Experiment	Calculation	τ = 1.07 sec	Equilibrium	Kinetics, $\tau = 10^{10}$ sec
$C_{16}H_{34}$	9.7	5.5	5.89	0	0
C_8H_{16}	1.2	1.8	0.07	0	0
C_9H_{18}	0.8	1.5	0.02	0	0
C_5H_{10}	4.3	3.8	1.25	0	0
C_6H_{12}	1.7	3.0	0.17	0	0
C_7H_{14}	1.2	2.3	0.08	0	0
$C_{10}H_{20}$	0.7	1.2	0	0	0
$C_{11}H_{22}$	0.6	0.9	0	0	0
$C_{12}H_{24}$	0.5	0.7	0	0	0
$C_{13}H_{26}$	0.4	0.5	0.03	0	0
$C_{14}H_{28}$	0.3	0.4	0.07	0	0
$C_{15}H_{30}$	0.2	0.2	0.03	0	0
C_2H_6	3.5	2.6	0.34	0.02	0.04
C_4H_8	5.5	4.9	9.67	0	0
C_3H_8	0.8	0.3	0.12	0	0
C_3H_6	14.8	15.5	26.95	0	0.03
C_2H_4	33.1	34.4	38.91	0.07	0.03
H_2	5.4	4.5	3.02	12.53	37.35
CH_4	12.9	13.8	12.01	65.27	37.06
C_3H_4	Not in list	Not in list	0.54	0	2.57
C_4H_6	–//–	–//–	0.48	0	0
C_2H_2	–//–	–//–	0.35	0	1.75
C_6H_6	0.2	–//–	0	21.87	0.01
C_4H_2	Not in list	–//–	0	0	20.44
Molecular mass of mixture	—	—	44.38	27.80	18.60

TABLE 3

Data	Methanol conversion, mole %	H_2	CO	CO_2	CH_4	CH_2O	C_2H_6
Experiment	2.1	2.1	0.077	0.923	Not in list	Not in list	Not in list
Kinetic model	2.6	0.726	0.056	0	0.163	0.778	0
Equilibrium	100	3.0	0.001	0.998	0.003	0	0
$\tau = 6.0$ sec	2.1	0.721	0.049	0	0.162	0.787	0

Notes. $T = 817.15$ K, $p = 246$ bar, and $\tau = 6.6$ sec. Initial concentration of methanol in supercritical water is $[CH_3OH] = 4.51 \cdot 10^{-3}$ mole/liter and $[O_2] < 0.04 \cdot 10^{-3}$ mole/liter.

TABLE 4

Data	Methanol conversion, mole %	H_2	CO	CO_2	CH_4	CH_2O	C_2H_6
Experiment	96.2	0.291	0.466	0.534	Not in list	Not in list	Not in list
Kinetic model	98.5	0.247	0.557	0.439	0.031	0.003	0
Equilibrium	100	0.845	0	1.0	0	0	0
$\tau = 1.4$ sec	96.2	0.129	0.636	0.356	0	0.008	0

Notes. $T = 798.15$ K, $p = 246$ bar, and $\tau = 9.6$ sec. Initial concentration of methanol in supercritical water $[CH_3OH] = 2.0 \cdot 10^{-3}$ mole/liter and $[O_2] = 3.49 \cdot 10^{-3}$ mole/liter.

TABLE 5

Data	Methanol conversion, mole %	H_2	CO	CO_2	CH_4	CH_2O	C_2H_6
Experiment	15.9	0	0.214	0.786	Not in list	Not in list	Not in list
Kinetic model	99.6	0.002	0.358	0.641	0	0.0006	0
Equilibrium	100	0	0	1.0	0	0	0
$\tau = 0.7$ sec	15.9	0.009	0.443	0.006	0	0.551	0

Notes. $T = 766.15$ K, $p = 246$ bar, and $\tau = 7.6$ sec. Initial concentration of methanol in supercritical water is $[CH_3OH] = 1.28 \cdot 10^{-3}$ mole/liter and $[O_2] = 3.48 \cdot 10^{-3}$ mole/liter.

with experimental data [11] and kinetics calculations by others [13]. Pyrolysis took place at $p = 160$ atm. The comparisons were done for equal conversions of the initial material. It is clear that, in terms of the composition and the pyrolysis time τ, the results of the computational models I and II and the model from [13] are similar and agree satisfactorily with experiment.

Figure 3 shows the results of a detailed kinetic calculation of butane pyrolysis under the same conditions using model I, as well as some experimental data from [11] and a local equilibrium calculation according to the model that we used before. The experimental data are close to the results for a local equilibrium and for the detailed kinetic model.

Table 2 shows a comparison of our calculations for cracking a mixture of n-hexadecane with water vapor at atmospheric pressure with calculated and experimental data [6]. The experiment was conducted under the following conditions: $T = 923$ K, $p = 1$ atm, $\tau = 1.07$ sec, and mass feed rates of $C_{16}H_{34}$ of 13.4 g/h and of H_2O of 39.5 g/h. The detailed kinetic scheme of [6], supplemented with reactions from [3], was used for the calculations. In all 69 substances and 908 reactions were considered, with the reactions with water neglected, as in [6]. The deviation from the experimental data on the concentration in the kinetic model was 2.38% for hydrogen and 0.89% for methane. It is clear from the data shown here that as the reaction time increases to $t = 10^{10}$ sec, there is an increase in the yields of hydrogen, methane, and the hydrogen-depleted compound C_4H_2, which, however, was not converted into benzene C_6H_6. In a calculation of the equilibrium state, the compound C_4H_2 is entirely converted into benzene; here the amount of hydrogen is reduced and the molecular mass of the hydrocarbon mixture changes. Note that, following the scheme of [6], we did not include carbon molecules in the reaction. With a long reaction period, the carbon in the compounds C_4H_2 and C_6H_6 can be transformed into pure carbon in both the kinetic and the equilibrium models.

The oxidation of methanol in supercritical water has been studied experimentally [14]. In a calculation using the detailed kinetic model we included 30 substances and 242 reactions. The kinetic parameters of the forward reactions were taken from [3] and those of the reverse reactions, by the methods described above. The calculations are compared with experiment in Tables 3–5. The last line of each table lists the time τ and composition of the products calculated by the kinetic model for a methanol conversion equal to that observed in the experiments. The concentrations of the reaction products are listed in the same form as in [14]: $C_i = x_i/(x_{(CH_3OH)_0} - x_{(CH_3OH)_f})$ [mole/mole], where $x_{(CH_3OH)_0}$ is the concentration of methanol in the initial mixture [mole/liter], $x(CH_3OH)_f$ is the concentration of methanol after the specified time, and x_i is the concentration of the given substance after this same time period. A number of experiments and calculations corresponding to them are listed in Tables 3–5.

An analysis of the experimental data in Tables 3–5 shows that the kinetic model gives 1.2–11 times higher rates of conversion than the experiments. In calculating the conversion of a mixture of n-hexadecane and water vapor at atmospheric pressure, the rate of conversion according to the expanded kinetic model is closer to the calculations of [6] than to experiment, and differs from the experimental results by almost a factor of two, while the briefer kinetic scheme gives a value of the conversion time that is closer to experiment. In choosing a chemical reaction scheme, one of the criteria for an adequate set of reactions is the degree of agreement between the equilibrium and kinetic calculations over sufficiently long reaction times. However, for high molecular reagents, no foreseeable system of reactions can be a complete system of possible reactions, so the kinetic calculations will give results that differ from equilibrium, even for very long reaction times. In addition, in real experiments fast reactions can be retarded by diffusion, when the diffusion time of the components that are formed is exceeded by the time for them to react among themselves and fluctuations occur in the reagent concentrations.

In the present paper, we have obtained qualitative and, in some cases, quantitative agreement between our calculations of the conversion time and of the reaction product composition and the experiments and calculations of others. More precise agreement between the calculations and experiment will require inclusion of the mixing of the reagents in the reactor, heat and mass transfer processes at the walls which influence the temperature level in the reactor, and other real processes that affect the rate of hydrocarbon conversion and the composition of the resultant products.

This work was supported by the Russian Foundation for Fundamental Research (Grant No. 97-02-18520).

REFERENCES

1. V. M. Glazov and L. M. Pavlova, *Chemical Thermodynamics and Phase Equilibria* [in Russian], Metallurgiya, Moscow (1988).
2. R. C. Reid, J. M. Prausnutz, and T. Sherwood, *The Properties of Gases and Liquids*, McGraw-Hill, New York (1977).
3. C. K. Westbrook and F. L. Dryer, "Chemical kinetic modeling of hydrocarbon combustion," in: *Prog. Energy Combust. Sci*, **10**, 1–57 (1984).
4. A. F. Dregalin, I. A. Zenukov, V. G. Kryukov, and V. I. Naumov, *Mathematical Modeling of High-Temperature Processes in Power Plants* [in Russian], Izd. Kazan' Univ., Kazan' (1985).
5. E. A. Moelwyn-Hughes, *The Chemical Statics and Kinetics of Solution*, Academic Press, London–New York (1971).
6. D. Depeyre and C. Flicoteaux, "Modeling of thermal stream cracking of *n*-hexadecane," *Ind. Eng. Chem. Res.*, **30**, 1116–1130 (1991).
7. H. R. Holgate, P. A. Webley, and J. W. Tester, "Carbon monoxide oxidation in supercritical water: The effects of heat transfer and water–gas shift reaction on observed kinetics," *Energy Fuels*, **6**, 586–597 (1992).
8. Yu. M. Zhorov, *Kinetics of Industrial Organic Reactions* [in Russian], Khimiya, Moscow (1989).
9. Yu. M. Zhorov, I. I. Vasil'eva, G. M. Panchenkov, and S. T. Kuz'min, "Mathematical description of the pyrolysis of benzenes," *Khim. Tekhnol. Topliv Masel*, No. 4, 16–19 (1975).
10. B. M. Fabuss, R. Kafesjian, J. O. Smith, and Ch. N. Satterfield, "Thermal decomposition rates of saturated cyclic hydrocarbons," *Ind. Eng. Chem.*, **3**, No. 3, 132–138 (1964).
11. H. J. Hepp and F. E. Frey, "Pyrolysis of propane and butanes at elevated pressure," *Ind. Eng. Chem.*, **45**, 410 (1953).
12. N. A. Vatolin, G. K. Moiseev, and B. G. Trusov, *Thermodynamic Modeling in High-Temperature Inorganic Systems* [in Russian], Metallurgiya, Moscow (1994).
13. R. G. Mallinson, R. L. Braun, C. K. Westbrook, and A. K. Burnham, "Detailed chemical kinetics study of the role of pressure in butane pyrolysis," *Ind. Eng. Chem. Res.*, **31**, 37–45 (1992).
14. J. W. Tester, P. A. Webley, and H. R. Holgate, "Revised global kinetic measurements of methanol oxidation in supercritical water," *Ind. Eng. Chem. Res.*, **32**, 236–239 (1993).